ISSN 0036-0244, Russian Journal of Physical Chemistry A, 2015, Vol. 89, No. 12, pp. 2243–2247. © Pleiades Publishing, Ltd., 2015.
Original Russian Text © A.E. Galashev, Yu.P. Zaikov, 2015, published in Zhurnal Fizicheskoi Khimii, 2015, Vol. 89, No. 12, pp. 1899–1903.

Computer Simulation of Li^+ Ion Interaction with a Graphene Sheet

A. E. Galashev[a] **and Yu. P. Zaikov**[b]
[a] *Institute of High Temperature Electrochemistry, Ural Branch, Russian Academy of Sciences, Yekaterinburg, 620137 Russia*
[b] *Yeltsin Ural Federal University, Yekaterinburg, 620002 Russia*
e-mail: alexander-galashev@yandex.ru

Received January 22, 2015

Abstract—The behavior of lithium ion in a flat channel formed by graphene sheets under the effect of an electrostatic field is studied by means of molecular dynamics. The optimum size of the gap between the sheets of graphene in which the movement of ions occurs with minimal deviation from the directions given by the field is found. The horizontal and vertical mobility of carbon atoms in each of the graphene sheets between which a lithium ion moves are calculated along with the stress tensor of the graphene channel, the σ_{zz}-component of which is most critical during the motion of the ion within the channel.

Keywords: graphene, lithium ion, channel, strain, mobility.

DOI: 10.1134/S0036024415120122

INTRODUCTION

Electrochemical devices for energy storage include, batteries, fuel cells, and supercapacitors. Graphene has high electric conductivity and strength, and supercapacitors based on it could find wide application in portable electronics. Porous graphene-based nanostructures with large surface areas could be used for their manufacture. However, the optimum pore size and distance between stacked graphene sheets remain undetermined. A simple statistical estimate of minimum distance h between two parallel graphene sheets that is favorable for the movement of metal ions without interference from the molecular force field was made in [1]. For lithium ions (Li^+), this value was 0.50 nm.

According to the authors of [1], the forces of attraction and repulsion acting on an Li^+ ion placed between sheets of graphene compensate for one another in the interplanar spacing range of 0.50 nm, and the ion moves in the gap as a free particle. In reality, however, the relief of the molecular force field of a graphene sheet is not flat. This forces the ion to perform microvibrations during its motion and deviate from the direction of the surrounding electrostatic field. The ion is strongly inhibited in the intrapalnar gaps with $h \approx 0.5$ nm, so considerable force is required to overcome the resistance of the molecular field. Such force can be created by an electric field of high strength. The h value must be determined in a rigorous dynamic model for each value of the field strength. Functionalization allows us to change the physical properties of graphene. With its metallization with lithium, charge transfer occurs from Li to C, resulting in a modified graphene that is able to retain hydrogen [2]. Due to the presence of dangling bonds, hydrogen adsorption can occur in the vicinity of defects present on the graphene or on its edges [3].

The adsorbed hydrogen in graphene creates an electrical charge of around $+0.21e$ [4]. Real graphene almost always contains defects, in the vicinity of which electrical charges appear and are retained. This can create additional obstacles for the movement of Li^+ ions between the graphene sheets. Contact between Li^+ ions and C atoms in graphene is necessary for the functioning of a graphene anode.

The aim of this work was to determine the shortest distance between sheets of perfect graphene on which Li^+ ions would move with minimal interference in a constant electric field, without losing contact with C atoms and thus being slowed by the graphene.

COMPUTER MODEL

Our calculations were performed using classical molecular dynamics (MD). The Tersoff potential was used as the basis of interactions in graphene [5, 6]:

$$U^{\mathrm{Ter}} = \frac{1}{2}\sum_i \sum_{j \neq i} f_c(r_{ij})\{f_R(r_{ij}) + b_{ij} f_A(r_{ij})\}, \qquad (1)$$

$$f_R(r) = A\exp(-\lambda_1 r),$$

$$f_c(r) = \begin{cases} 1, & r < R, \\ \frac{1}{2} + \frac{1}{2}\cos\frac{\pi(r-R)}{S-R}, & R < r < S, \\ 0 & r > S, \end{cases}$$

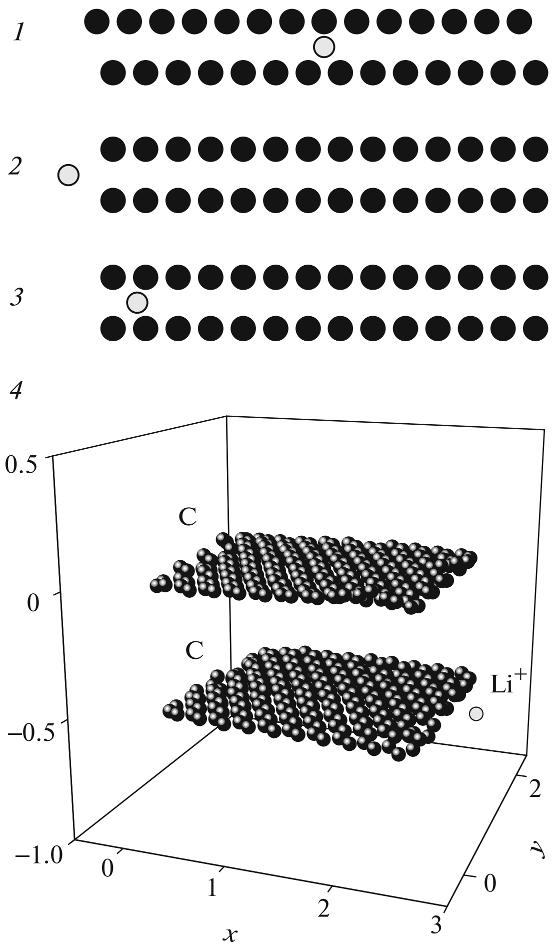

Fig. 1. Scheme of the atoms' arrangement at time $t = 0$: (*1*) view of the frontal plane; (*2, 3*) side view (on $x0z$ plane) of the external and internal location of an Li^+ ion in channel, respectively; (*4*) flat channel of graphene–lithium ion system configuration at moment 100 ps and $h = 0.60$ nm. The electric field intensity is directed along axis $0x$. Initially, the Li^+ ion is located at the front of plane $y0z$ outside the channel. Distances are given in nm.

$$f_A(r) = -B\exp(-\lambda_2 r),$$

$$b_{ij} = \left(1 + \beta^n \varsigma_{ij}^n\right), \ \varsigma_{ij} = \sum_{k \neq i,j} f_c(r_{ik}) g(\theta_{ijk}),$$

$$g(\theta) = 1 + \frac{c^2}{d^2} - \frac{c^2}{d^2 + (h - \cos\theta)^2}.$$

Carbon atoms are denoted here by indices i, j, k; r_{ij} is the bond length; and θ_{ijk} is the angle between bonds i–j and j–k. The parameters of the Tersoff and Lennard-Jones potentials are used below to represent C–C and Li–C interactions [1, 5, 7, 8]:

$A = 1393.6$ eV, $B = 346.7$ eV, $\lambda_1 = 3.4879$ nm^{-1}, $\lambda_2 = 2.2119$ nm^{-1}, $\lambda_3 = 0$ nm^{-1}, $n = 0.72751$, $c = 3.8049 \times 10^4$, $d = 4.384$, $R = 0.18$ nm, $S = 0.23$ nm, $\beta = 1.5724 \times 10^{-7}$, $h = -0.57058$, $\sigma_{\text{C–C}}^{LJ} = 0.34$ nm, $\varepsilon_{\text{C–C}}^{LJ} = 2.84$ meV, $\sigma_{\text{Li–C}}^{LJ} = 0.2473$ nm, $\varepsilon_{\text{Li–C}}^{LJ} = 4.33$ meV.

The modeling of two-dimensional systems (e.g., graphene) with a covalent bond requires modification of the potential [7]. In this model, the maximum coverage (S) of covalent interactions is increased from 0.21 to 0.23 nm [8]. Beyond the limits of covalent interaction, there is a weak Lennard-Jones interaction that has the property of attraction. The parameters of Lennard-Jones potentials $\sigma_{\text{C–C}}^{LJ}$ and $\varepsilon_{\text{C–C}}^{LJ}$ taken from [7] are given above. To prevent rotation of the graphene sheet, braking in each atomic node of graphene was applied with a force of $-dV_{ij}(\Omega_{kijl})/dr_{ij}$, where torque potential $V_{ij}(\Omega_{kijl})$ was defined as in [7]. The interaction between a lithium ion and carbon atoms were represented by the Lennard-Jones potential with parameters of $\sigma_{\text{Li–C}}^{LJ}$ and $\varepsilon_{\text{Li–C}}^{LJ}$ taken from [1] (see above).

Our sheets of graphene contained 406 atoms and were rectangular in shape at 3.4 × 3 nm (the sheet had 14 atoms along each edge). The high capacity of the electrode is achievable upon the rapid movement of electrolyte ions, so the self-diffusion coefficient of the ion would lay within the range of 10^{-10} to 10^{-13} cm^2/s [9]. In preliminary computer experiments with a gap of 0.50–0.65 nm between the graphene sheets, we showed that this effect was achieved starting from a value of electric field intensity close to 10^3 V/m. A constant electric field with an intensity of 10^3 V/m accelerated Li^+ ions along axis ox oriented along the zigzag direction of the graphene sheets. The graphene sheets were arranged in accordance with Bernal laying (ABAB...) in exactly the same manner as in bulk graphite. The gap of value h was set between the two parallel sheets of graphene. Two series of calculations were performed that corresponded to schemes *1–2* and *1–3* (Fig. 1). In the first series, an Li^+ ion at the initial moment in time was in front of the gap formed by graphene sheets at a distance of $\sigma_{\text{Li–C}}^{LJ}$ from the front boundary of the gap (with plane $y0z$ passing through the front edges of the sheets). A point located in the channel at a distance from the virtual frontal plane (defined by the entrance to the channel) served as the initial position of the center of the ion in the second series of calculations. Each series consisted of four calculations with a duration of 1 million time steps $\Delta t = 1 \times 10^{-16}$ s with different values of h. Values of $h = 0.50$, 0.55, 0.60, and 0.65 nm were used. For both series, the initial location of the ion corresponded to a height of $h/2$. At $t = 0$, the ion was in front of or right near the middle of the plate's channel formed by zigzag rows of atoms of the lower graphene membrane (Fig. 1).

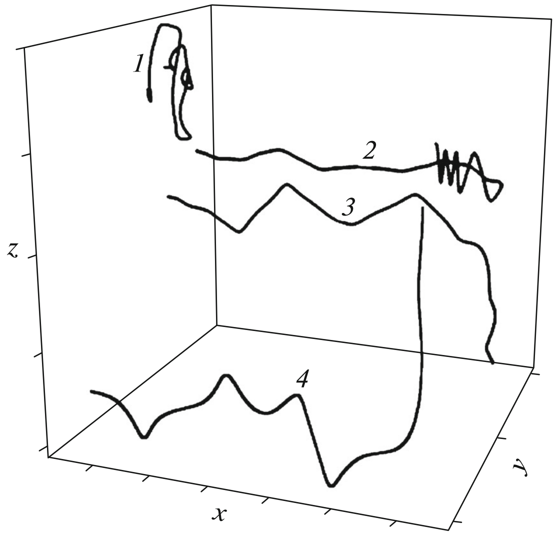

Fig. 2. Trajectories of the lithium ion in a flat channel of graphene with a gap of (*1*) 0.50, (*2*) 0.55, (*3*) 0.60, (*4*) 0.65 nm.

Even though the interaction between parallel graphene sheets fell rapidly as the distance between them grew and almost completely disappeared in the investigated range of distances (0.50–0.65 nm), the Li^+ ion was not free to move in the interplanar gap. This was because strong covalent bonds acting in the plane of the graphene allowed only slight warpage vibration of sheets during the Li^+ ion's motion. Affected by the Van der Waals interaction with close-packed C atoms of graphene sheets, the Li^+ ion decelerated.

The self-diffusion coefficient is given by the mean square of atomic displacement $\left\langle[\Delta\mathbf{r}(t)]^2\right\rangle$ [10]:

$$D = D_{xy} + D_z = \lim_{t\to\infty}\frac{1}{2\Gamma t}\left\langle[\Delta\mathbf{r}(t)]^2\right\rangle, \qquad (2)$$

where $\Gamma = 3$ is the dimension of the space. Averaging over time is denoted by $\langle\ldots\rangle$.

To calculate the strains that occur in the graphene sheet, it was divided into elementary areas. Atomic strains $\sigma_J(l)$ on a elementary square with number l for each of the directions x, y, z with current index J were determined by calculating the kinetic energies of the atoms in that area and the projections of the forces acting on l square by all other atoms [11]:

$$\sigma_J(l) = \left\langle\sum_i^k \frac{1}{\Omega}\left(m v_J^i v_J^i\right)\right\rangle + \frac{1}{S_l}\left\langle\sum_i^k\left(f_J^i\right)\right\rangle, \qquad (3)$$

where k is the number of atoms on area l; Ω is the volume per atom; m is atomic mass; v_J^i is the J-projection of the velocity of atom i; and S_l is the area of square l.

RESULTS AND DISCUSSION

An ion in front of the entrance to the channel passes over the length of the graphene sheet by moment in time 100 ps when the gap is 0.60 or 0.65 nm wide. Coming out of the channel, the ion does not travel too far from it; instead, it is attracted to the lower sheet of graphene, indicating there is tangible interaction between C atoms and the ion (Fig. 1).

The trajectories of an Li^+ ion in front of a flat graphene channel and moving under the effect of a constant electric field with an intensity of 10^3 V/m are shown in Fig. 2. For the detection of transverse oscillations during the ion's movement, the scale on the vertical axis (z) was stretched about 4 times. When the gap was 0.50 nm, the ion was unable to enter the channel and described looping trajectories directly in front of the channel. Increasing the interplanar gap to 0.55 nm drastically altered the ion's pattern of movement. Translational motion became dominant. With small smooth oscillations, it reached the opposite end of the channel, where it was slowed by C atoms. It then performed an oscillating translational motion in the opposite direction. The resistance from the C atoms finally exceeded that of the inertia of the decelerated ion, preventing it from leaving the channel. The movement of the Li^+ ion along the channel under the constant electric field was due to the presence of an energy barrier to inertial movement both at the entrance and the exit of the channel. Increasing the gap even more (to 0.60 nm) allows the ion to travel the length of the channel. Low-frequency quasi-periodic oscillations are superimposed on the translational motion of the ion. The amplitude of these oscillations is much larger than before. The trajectory of the ion leaving the channel is deflected downward. Further expansion of the gap (to 0.65 nm) does not appreciably alter the path of the Li^+ ion in the channel. The ion in this case performs aperiodic oscillations and flies upward upon exiting the channel.

The deceleration effect of the relief of the molecular field becomes apparent when we consider that in the time of 100 ps, the Li^+ ion inside the gap traveled only 0.40 and 1.18 nm in the direction of an electric field with an intensity of 10^3 V/m when the gap was 0.50 and 0.55 nm, respectively. If the starting point of the ion's trajectory lies within the channel when the gap is 0.60 nm, the Li^+ ion passes through the channel in 100 ps; with a gap of 0.65 nm, it remains in the space between the sheets because of the abrupt change in its path of movement before exiting the channel. From the standpoint of effective control of an ion's motion along the channel using a constant electric field with intensity of 10^3 V/m, it is thus most expedient to use a gap of 0.60 nm between the sheets of graphite.

Let us now consider the effect the gap has on the kinetic and mechanical properties of the graphene

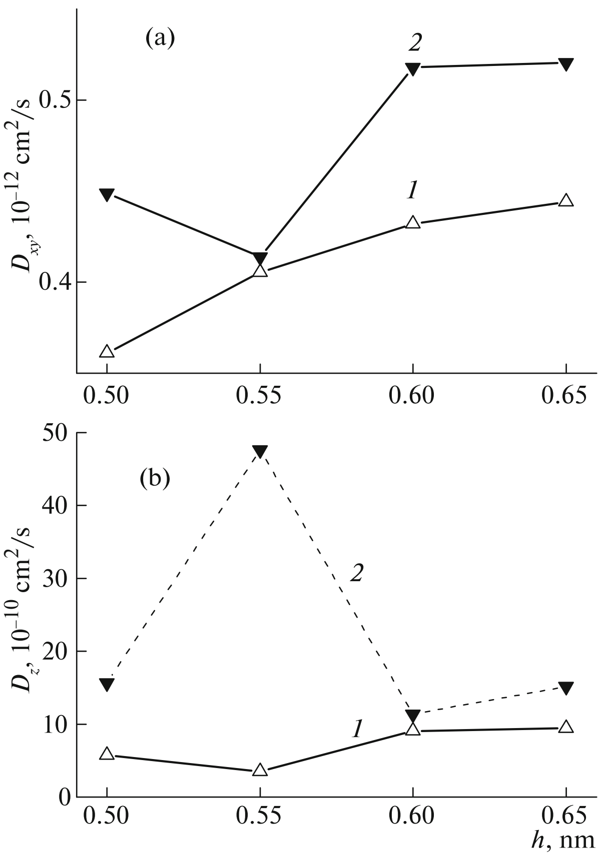

Fig. 3. Coefficients of the (a) horizontal and (b) vertical mobility of graphene atoms in the (*1*) lower and (*2*) upper sheets forming a flat channel. At $t = 0$, the Li^+ ion was at the front of plane $y0z$ of the channel.

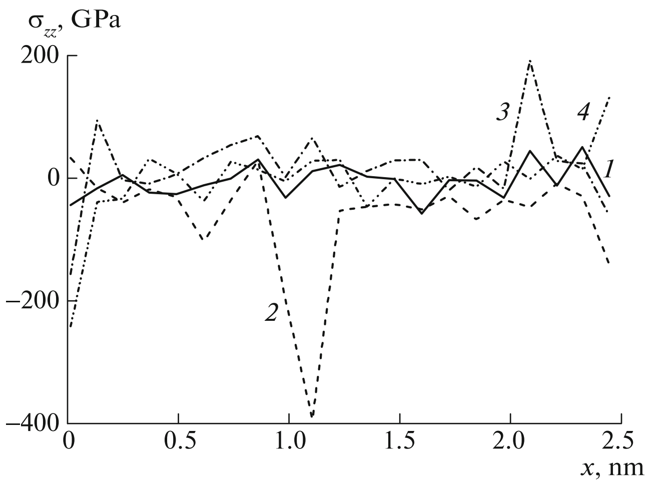

Fig. 4. Distribution of strain $\sigma_{zz}(x)$ averaged over both sheets of graphene along axis $0x$ (zigzag direction) coinciding with the direction of the electric field strength at gaps of (*1*) 0.50, (*2*) 0.55, (*4*) 0.60, and (*3*) 0.65 nm.

sheets themselves when the ion is outside the flat channel at $t = 0$. The initial localization of the ion within the channel leads to identical conclusions. Considering the geometry of the system, it is advisable to investigate the behavior of the horizontal D_{xy} and vertical D_z components of the mobility factor of C atoms in graphene separately. The values of these components at different values of the gap are shown in Fig. 3. With an increase in the gap, component D_{xy} for the lower graphene sheet grows continuously (Fig. 3a, curve *1*), while the dependence of D_{xy} for the top sheet (curve *2*) has a minimum at $h = 0.55$ nm. In general, the horizontal mobility of the atoms in the top sheet of graphene is greater than in the lower sheet. The reduction in the horizontal mobility of the atoms in the upper graphene sheet and the slight decrease in the vertical mobility of the atoms in the lower sheet when $h = 0.55$ nm are compensated for by a considerable increase in the value of D_z for the upper graphene sheet at this size of gap. Strong fluctuations in the mobility of the atoms in this case indicate the Li^+ ion finds it difficult to move within the interplane gap. When $h = 0.60$ nm, the vertical mobility of the atoms of the lower and upper sheets of graphene approach each other most strongly. The average values of D_{xy} and D_z for these sheets are somewhat lower than when $h = 0.65$ nm. The low values of D_z at relatively high values of D_{xy} for both graphene sheets begin at the gap size of 0.60 nm and are maintained at a gap of 0.65 nm. These conditions are favorable for the movement of the ion within the channel. Consequently, the gap of $h = 0.60$ nm may be considered optimal for the motion of a Li^+ ion in a flat graphene channel.

The distribution of the greatest strains σ_{zz} in the graphene sheets (lower and upper combined) along axis $0x$ (the zigzag direction) is shown in Fig. 4 for four values of the intersheet gap. Increasing the gap slows the rate at which the Li^+ ion enters the channel (due to weakening of the attraction of C atoms). The decelerated ion is deflected more strongly by the molecular force field. This results in more pronounced fluctuations of σ_{zz} at the entrance to the channel when $h = 0.60$ and 0.65 nm. For free two-layer graphene, the fluctuations of function $\sigma_{zz}(x)$ do not exceed ±50 GPa [12–14]. This range also fits the oscillations of function $\sigma_{zz}(x)$ when an Li^+ ion moves between sheets of graphene with a gap $h = 0.50$ nm. Increasing the gap leads to increased fluctuations. In the range of $x \approx 1.1$ nm at $h = 0.55$ nm, particularly strong fluctuations are observed due to the considerable deflection of the Li^+ ion upward. The ion is decelerated near the exit of the channel, further strengthening the $\sigma_{zz}(x)$ fluctuations. The optimum size of the gap between the planes does not prevent moderate stains from arising in the graphene sheets.

Let us note the main differences associated with changes in the location of the initial point of the trajectory of the Li^+ ion. The vertical mobility of carbon atoms is almost identical for both ways of introducing the ion. The horizontal mobility of C atoms differs appreciably only at the smallest value of the gap, i.e., when $h = 0.50$ nm. They have lower values for both the lower and the upper graphene sheet when the Li^+ ion is outside the channel at the initial point in time. Strains σ_{zz} that arise in the graphene sheets are generally not strongly dependent on the location of the Li^+ ion at time $t = 0$. An exception is when $h = 0.50$ nm, where stronger positive strains emerge at the entrance and negative strains as strong as the first arise at the exit when a Li^+ ion is introduced into the channel.

CONCLUSIONS

The behavior of lithium ion in a flat channel formed by graphene sheets under the influence of a constant longitudinal electric field was studied. The characteristic changes occurring in graphene upon the movement of an ion were established. The obtained results will be valuable in designing graphene anodes for electrochemical supercapacitors and batteries.

REFERENCES

1. Y. Chan and J. M. Hill, Micro Nano Lett. **5**, 247 (2010).
2. C. Ataca, E. Akturk, S. Ciraci, and H. Ustunel, Appl. Phys. Lett. **93**, 043123 (2008).
3. F. D. Lamari and D. Levesque, Carbon **49**, 5196 (2011).
4. E. Rangel, G. Vazquez, F. Magana, and E. Sansores, J. Mol. Model. **18**, 5029 (2012).
5. J. Tersoff, Phys. Rev. B: Condens. Matter **39**, 5566 (1989).
6. A. E. Galashev, V. A. Polukhin, I. A. Izmodenov, and O. R. Rakhmanova, Glass Phys. Chem. **33**, 86 (2007).
7. S. J. Stuart, A. V. Tutein, and J. A. J. Harrison, Chem. Phys. **112**, 6472 (2000).
8. A. E. Galashev and V. A. Polukhin, Russ. J. Phys. Chem. A **88**, 995 (2014).
9. B. Peng, F. Cheng, Z. Tao, and J. Chen, J. Chem. Phys. **133**, 034701 (2010).
10. A. E. Galashev and V. A. Polukhin, Phys. Met. Metallogr. **115**, 697 (2014).
11. A. E. Galashev, Tech. Phys. **59**, 467 (2014).
12. A. E. Galashev and O. R. Rakhmanova, High Temp. **52**, 374 (2014).
13. A. E. Galashev, High Temp. **52**, 633 (2014).
14. A. E. Galashev and O. R. Rakhmanova, Phys. Usp. **57**, 970 (2014).

Translated by A. Pahigreva